Published in final edited form as:
Brain Res. 2010 July 9; 1343: 54–65. doi:10.1016/j.brainres.2010.04.066.

A neuroanatomical and physiological study of the non-image forming visual system of the cone-rod homeobox gene (*Crx*) knock out mouse

Louise Rovsing[a], **Martin F. Rath**[a], **Casper Lund-Andersen**[a], **David C. Klein**[b], and **Morten Møller**[a,*]

Morten Møller: morm@sund.ku.dk

[a]Department of Neuroscience and Pharmacology, Panum Institute, University of Copenhagen, Copenhagen, Denmark

[b]Section on Neuroendocrinology, Program in Developmental Endocrinology and Genetics, Eunice Kennedy Shriver National Institute of Child Health and Human Development, National Institutes of Health, Bethesda, MD, USA

Abstract

The anatomy and physiology of the non-image forming visual system was investigated in a visually blind cone-rod homeobox gene (*Crx*) knock-out mouse ($Crx^{-/-}$), which lacks the outer segments of the photoreceptors. We show that the suprachiasmatic nuclei (SCN) in the $Crx^{-/-}$mouse exhibit morphology as in the wild type mouse. In addition, the SCN contain vasoactive intestinal peptide-, vasopressin-, and gastrin-releasing peptide-immunoreactive neurons as present in the wild type. Anterograde *in vivo* tracings from the retina of the $Crx^{-/-}$ and wild type mouse showed that the retinohypothalamic projection to the SCN and the central optic pathways were similar in both animals. Telemetric monitoring of the running activity and temperature revealed that both the $Crx^{-/-}$and wild type mouse exhibited diurnal rhythms with a 24-h period, which could be phase changed by light. However, power spectral analysis revealed that both rhythms in the $Crx^{-/-}$ mouse were less robust than those in the wild type. The normal development of the SCN and the central visual pathways in the $Crx^{-/-}$ mouse suggests that a modulatory input from the photoreceptors in the peripheral retina to the retinal melanopsin neurons or the SCN may be necessary for a normal function of the non-image forming system of the mouse. However, a change in the SCN of the $Crx^{-/-}$ mouse might also explain the observed circadian differences between the knock out mouse and wild type mouse.

Keywords

Circadian; Melanopsin; Suprachiasmatic; Activity; Temperature

1. Introduction

The cone-rod homeobox gene *Crx* encodes a homeodomain transcription factor required for expression of photoreceptor specific genes in the mammalian retina (Chen et al., 1997; Furukawa et al., 1997; Peng and Chen, 2007) and is important for development and maintaining of the photoreceptors (Furukawa et al., 1999; Nishida et al., 2003; Rath et al.,

*Corresponding author. Department of Neuroscience and Pharmacology, Panum Institute, room 24.3.43, Blegdamsvej 3, 2200 København N, Denmark.

2007). *Crx*$^{-/-}$ mouse was generated by Furukawa et al. (1999) by a targeted disruption of the *Crx* homeobox. The *Crx*$^{-/-}$ mouse is visually blind due to the lack the outer segments of the photoreceptors (Furukawa et al., 1999; Morrow et al., 2005).

The retinal rods and cones are the classical photoreceptors of the visual system of vertebrates. The visual system has been shown to consist of an image-forming visual system, which enables the animal to detect and trace objects in the visual world, and a non-image forming visual system (David-Gray et al., 1998; Doyle and Menaker, 2007) detecting ambient luminance, which synchronizes the animal's biological clock with the circadian day-night cycle. This system involves direct light sensitive melanopsin containing retinal ganglion cells (Panda et al., 2003; Provencio et al., 2009) and controls, via entraining the suprachiasmatic nuclei (SCN) in the hypothalamus (Morin, 1994), circadian hormone secretion and synthesis, locomotor activity and also the pupil size (Czeisler et al., 1995; Foster and Hankins, 2002; Fu et al., 2005).

The SCN is the biological clock of vertebrates (Korf etal., 2003; Doyle and Menaker, 2007). Neurons in the SCN express clock genes responsible for the generation of the circadian rhythms (Foster, 1998; Okamura, 2004); the rhythmic output from these neurons is entrained by the retina via the retinohypothalamic tract (Hannibal et al., 2000) and is projected to other parts of the central nervous system (Vrang et al., 1995; Munch et al., 2002) regulating the circadian activity in these target areas. These target areas include the paraventricular nucleus of the hypothalamus (Vrang et al., 1995) involved in release of corticotrophin releasing factor (Jessop et al., 1989), the dorsal subparaventricular hypothalamic area participating in the regulation of body temperature (Chou et al., 2002), and the ventral subparaventricular area involved in sleep regulation (Saper et al., 2005). Finally, the SCN controls the melatonin production in the pineal gland (Klein et al., 1997), which is targeted via a multisynaptic pathway involving the paraventricular nucleus (Klein et al., 1983; Yanovski et al., 1987; Vrang et al., 1995) and the peripheral sympathetic nervous system (Kappers, 1960; Larsen et al., 1998; Møller and Baeres, 2002).

The retinal ganglion cells containing the photopigment melanopsin are directly light sensitive (Berson et al., 2002; Hattar et al., 2002; Warren et al., 2003; Hankins et al., 2008) and axons from these perikarya innervate neurons of the ventral part of the SCN via the retinohypothalamic tract (Hattar et al., 2002). However, the melanopsin-containing neurons of the inner retina are connected with the photoreceptors of the outer retina, and rods and cones influence the activity of the melanopsin-containing ganglion cells of the inner retina (Freedman et al., 1999; Viney et al., 2007). Functionally, rodents with degenerate rods and cones retain the ability to phase-shift in response to light (Foster and Soni, 1998; Semo et al., 2003; Tosini et al., 2007); however, mice lacking melanopsin can still be photoentrained, although the response to light becomes subnormal (Lucas et al., 2003; Ruby et al., 2002; Panda et al., 2002). This indicates that photodetection in both the outer and inner retina influences circadian timing. In a recent study it was shown that the CBA/J mouse, which is characterized by a degenerate photoreceptor layer and attenuated phase-shifting responses, has a normal distribution of melanopsin-containing retinal ganglion cells and that these cells also exhibit a normal dendritic pattern in the retina (Ruggiero et al., 2009). The attenuated phase-shifting in these animals might be explained by changes in the innervation of the SCN, endogenous changes in the SCN itself or some of the central visual pathways.

In this context, the generation of the *Crx*$^{-/-}$ mouse (Furukawa et al., 1999) has made it possible to study the involvement of the outer retina in the non-image forming system of the mouse. *Crx* encodes a homeodomain transcription factor which regulates tissue-specific gene expression in the retinal photoreceptors and the pineal gland (Chen et al., 1997; Furukawa et al., 1997). In *Crx*$^{-/-}$ mice, the outer segments of the photoreceptors do not

develop, and in the adult retina of the *Crx*$^{-/-}$ mouse, the outer nuclear layer is reduced to 2–3 rows of nuclei (Furukawa et al., 1999; Nishida et al., 2003). Accordingly, the *Crx*$^{-/-}$ mouse is blind and the electroretinograms of the *Crx*$^{-/-}$ show a reduction of the rod ERG to less than 1% and cone activity is undetectable; the mice further show retinal reduction in rhodopsin and cone opsins (Furukawa et al., 1999).

We have, therefore, in this study investigated the SCN and central visual pathways in the *Crx*$^{-/-}$ mouse, where rods and cones are genetically ablated. Analysis of the SCN as well as mapping of the visual pathways by in vivo neuronal tracing revealed no changes in the *Crx*$^{-/-}$ mice as compared to the wild type. Telemetric recordings of the circadian locomotor activity and temperature showed that both parameters exhibited circadian rhythms with a period of 24 h. However, the rhythms of the *Crx*$^{-/-}$ mouse were less robust than those of the control mice. These data suggest that the changes in circadian rhythmicity observed in the *Crx*$^{-/-}$ mouse are directly due to the degenerate retina; alternatively, these may reflect biochemical changes in the SCN not detected in this study.

2. Results

2.1. The homozygous *Crx*$^{-/-}$ mice undergo degeneration of the outer segments of the rods and cones, but melanopsin-immunoreactive neurons are present in the ganglion cell layer

The retina of the wild type mouse exhibited in toluidine blue stained sections a normal ten layered pattern (Fig. 1A); contrarily, the retina of the *Crx*$^{-/-}$ mouse exhibited degeneration of the outer segments of the photoreceptors, and the outer nuclear layer contained fewer nuclei than that in the control animals (Fig. 1B). This is in agreement with previous studies (Furukawa et al., 1999).

Melanopsin-immunoreactive neurons with processes extending to the inner nucleus layer were present in both the wild type (Fig. 1C) and the *Crx*$^{-/-}$ mouse (Fig. 1D).

2.2. The suprachiasmatic nuclei exhibit a normal morphology in the *Crx*$^{-/-}$ mouse and contain neurons immunoreactive for VIP, GRF, and vasopressin

2.2.1. Nissl staining—In coronal sections of the hypothalamus at the level of the optic chiasm, a classical drop shaped bilateral suprachiasmatic nucleus was present both in the wild type mouse (Fig. 1E) and in the *Crx*$^{-/-}$ mouse (Fig. 1F).

2.2.2. Immunohistochemistry—The suprachiasmatic nuclei of both the *Crx*$^{-/-}$ mouse (Fig. 2A, B, and C) and the wild type (Fig. 2D, E, and F) showed a normal immunoreactivity for gastrin releasing peptide (GRP) (Fig. 2A and D), vasoactive intestinal peptide (VIP) (Fig. 2B and E), and vasopressin (Fig. 2C and F). GRP-immunoreactivity was seen in perikarya, mostly in the ventral part of the nuclei, and in fibers throughout the nuclei. A strong VIP-immunoreactivity was present in perikarya and nerve fibers in all parts of the nuclei. Vasopressin immunoreactive perikarya were present in the dorso-medial and the ventrolateral part of the nuclei.

2.3. The optic system of the brain develops normally in the *Crx*$^{-/-}$ mouse

In the wild type and the *Crx*$^{-/-}$ mouse, the cholera toxin tracer was transported rapidly from the eye into the optic visual pathways. Thus, in both animals the tracer was observed in the superior colliculus 12 h after injection into the eyes (Fig. 3C and F).

In the wild type and the *Crx*$^{-/-}$ mouse, a dense terminal field was present bilaterally in the SCN (Fig. 3A and D). More caudal in the brain, a strong terminal field was present in the lateral geniculate nucleus contralateral to the injection site (Fig. 3B and E) with a dense

innervation of both the ventral and dorsal subnuclei and the intergeniculate leaflet. On the ipsilateral side of the injection, the dorsal and ventral lateral geniculate nuclei were labelled (Fig. 3C), but the terminal fields were smaller than on the contralateral side.

On both the ipsilateral and contralateral side, labeling was present in the pretectal nucleus of the wild type and *Crx*$^{-/-}$mouse. However, the optic pretectal nucleus was only labelled ipsilateral to the injection (Fig. 3C). All the superficial layers of the superior colliculus (Fig. 3C and F) were labeled on the contralateral injection side (Fig. 3C and F). Contrarily, a weak labeling of the deep layers was present on the ipsilateral side.

2.4. Telemetric analysis of activity and temperature rhythms in *Crx*$^{-/-}$ and wild type mouse

2.4.1. Activity rhythms—The locomotor activity rhythm of the wild type and the *Crx*$^{-/-}$ mouse kept in 12L:12D was monitored over a period of 20 days (Fig. 4). Both the wild type and the knock out mouse exhibited a prominent circadian locomotor activity. However, the amplitude of the *Crx*$^{-/-}$ mouse was considerable lower than that in the wild type (Fig. 4). By using the TSA Serial Cosinor test with 24 h chosen as the period, it was shown that the activity data could be fitted to a cosine curve with a period of 24 h (Table 1); both the mesor and the amplitude (Table 1) were lower in the *Crx*$^{-/-}$ mouse (mesor = 2.63) than in the wild type (mesor=11.7). Representative actograms of the locomotor activity of a wild type and a *Crx*$^{-/-}$ mouse (Fig. 5) show that the activity rhythm of the knock out mouse is most irregular with several smaller activity periods during the light period. By use of Lomb and Scargle power spectrum analysis of the periods (Lomb, 1976; Scargle, 1982), it was verified that both the wild type (Fig. 6A) and *Crx*$^{-/-}$ mice (Fig. 6C) showed a rhythm with a 24-h period, but that the power of the wild type animals is stronger (power = 82) than that of the *Crx*$^{-/-}$ mouse (power = 11).

When the mice were kept in constant light (Fig. 6E and G), the activity rhythm became irregular and the Lomb–Scargle power spectrum analysis did not reveal any statistical significant activity rhythms in either strain.

Finally, if the animals were exposed to constant darkness (Fig. 6I and L), the activity rhythm of the wild type (Fig. 6I) mouse showed a circadian rhythm with a period of 24 h. However, the period for the *Crx*$^{-/-}$ mouse (Fig. 6L) was 25 h and the power spectrum value was much lower (power = 18) than in the wild type (power = 44).

2.4.2. Temperature rhythms—The temperature rhythms were monitored in a wild type and *Crx*$^{-/-}$ mouse kept in 12L:12D over a period of 20 days (Fig. 7). Both the wild type and knock out mouse had a prominent circadian temperature rhythm. By analyzing the data by TSA Serial Cosinor test with 24 h chosen as the period, it was confirmed that neither the mesor of the temperature curve nor the amplitude (Table 1) were statistically different between the wild type (mesor: 36.4 °C) and the *Crx*$^{-/-}$ mouse (mesor: 36.3 °C). Plotting a periodogram of the temperature rhythms of a representative control and a *Crx*$^{-/-}$ mouse (Fig. 8) showed that the rhythm of the knock out mouse was slightly more irregular than the rhythm in the control mouse. This was verified by use of Lomb and Scargle power spectrum analysis, which showed that both the wild type (Fig. 6B) and the *Crx*$^{-/-}$ mouse (Fig. 6D) exhibited a rhythm with a 24-h period, but that the power of the wild type animals was stronger (power=139) than in the *Crx*$^{-/-}$ mouse (power = 22).

When the mice were kept in constant light, the temperature rhythm of the wild type animal exhibited a slightly prolonged period of 25 h (Fig. 6F), but the power of the rhythm indicated this to be less robust than observed in the 12L:12D regime. Contrarily, the temperature rhythm of the *Crx*$^{-/-}$ mouse was abolished during constant light (Fig. 6H).

When the animals were exposed to constant darkness (Fig. 6K and M), the temperature rhythms of the wild type regained a regular circadian rhythm with a period of 24 h (Fig. 6K). However, the period for the *Crx*$^{-/-}$ mouse (Fig. 6M) was now 25 h and the power spectrum value was lower than in the control mouse.

3. Discussion

Our investigations in this paper show that the visual blind *Crx*$^{-/-}$ mouse, in addition to a circadian activity rhythm also exhibits a circadian temperature rhythm, which can be phase changed by light.

The presence of a diurnal 24h activity rhythm and the phase change of this rhythm by light are in accordance with the previously published recordings in *Crx*$^{-/-}$ and wild type mice (Furukawa et al., 1999). In the current study, however, a detailed telemetric registration of the circadian rhythms of *Crx*$^{-/-}$ mice and the following Lomb-Scargle power spectrum analysis, showed that both temperature and activity rhythms were less robust in the *Crx*$^{-/-}$ mouse (exhibited lower frequency “power” of the dominant period) compared to the wild type. The Lomb-Scargle algorithm has several computational advantages over more common approaches, such as Fourier analysis, partly because it is less sensitive to random data and has known statistical properties (Glynn et al., 2006).

The less robust activity and temperature rhythms in the *Crx*$^{-/-}$ mice might have been due to lack of expression of melanopsin in the ganglionic cells of the retina. However, as shown in this study, melanopsin immunoreactive ganglionic cells are present in the retina of the *Crx*$^{-/-}$ mouse, but we have not yet studied possible quantitative differences between the knock out mouse and wild type. In a recent study of a mouse with degenerative outer retina, the CBA/J mouse, (Ruggiero et al., 2009), the loss of rods and cones in this mutant did not influence the number of melanopsin-containing neurons in the retina.

The less robust activity and temperature rhythms observed in the *Crx*$^{-/-}$ mice compared to the wild type mice might also be due to variation in innervation of the suprachiasmatic nuclei or in the development of central visual pathways of the brain. However, our *in vivo* tracings from the retina showed that the SCN of the *Crx*$^{-/-}$ mouse possesses a dense innervation from the retina, which did not differ from the innervation in the wild type. The innervation of the SCN from the retina in the wild type mouse has been described in previous tracing studies (Abrahamson and Moore, 2001; Hattar et al., 2006) and exhibit the same pattern as described by us in this study. Further, the morphology of the SCN as well at the content of classical neuropeptides such as gastrin releasing peptide, vasoactive intestinal peptide, and vasopressin did not differ in the *Crx*$^{-/-}$ mouse from the wild type. However, this does not exclude the possibility that the genotype of the SCN in the *Crx*$^{-/-}$ – is different from the wild type.

An interesting finding of this study relates to the observation that a 24-h temperature rhythm was maintained in constant light in the wild type mouse, whereas this was not seen in the *Crx*$^{-/-}$ mouse. Temperature is controlled by neurons in the medial preoptic region (Saper et al., 2005). The SCN connects to the preoptic regions via caudal projecting fibers to the dorsal subparaventricular region in the hypo-thalamus (Chou et al., 2003) and from there to the medial preoptic region (Chou et al., 2002). Lesion of the SCN abolishes the diurnal temperature rhythm (Refinetti, 1995; Scheer et al., 2005), but the anatomical projections from the SCN regulating activity are different from the projections regulating temperature (Abrahamson and Moore, 2001; Lu et al., 2001). Accordingly, our data suggest that the latter system regulating circadian changes in temperature is more vulnerable in an animal without functional photoreceptors (Chou et al., 2003).

4. Conclusions

In summary, this study shows the presence of light-entrain-able activity and temperature rhythms in the *Crx*$^{-/-}$ mouse in spite of the lack of rods and cones in the outer retina. However, both rhythms are less robust in the *Crx*$^{-/-}$ mouse than in the wild type. This difference does not appear to be associated with gross changes in the morphology of the SCN, innervation via the retinohypothalamic projection, or peptide transmitter levels in the SCN. Accordingly, on this basis, one can hypothesize that the input from the melanopsin system of the retina receives input from the retinal rods and cones, and that in the absence of this input, the output to the SCN is altered. Alternatively, it is possible that there is a direct effect of a retinally derived factor on the SCN, in a manner similar to that described for effects of retinally derived Otx2 homeodomain protein on the visual cortex (Sugiyama et al., 2008) or that the intrinsic molecular profile of the SCN in the *Crx*$^{-/-}$ might differ from the wild type.

5. Experimental procedures

5.1. Animals

Adult C57BL/6J male mice (20–30 g) were obtained from Charles River, Würtzburg, Germany. *Crx*$^{-/-}$ mice were generously provided to David C. Klein by Dr. Connie Cepko; animals used in this study were transferred from the National Institutes of Health, Bethesda, MD, and bred at the Panum Institute, University of Copenhagen, Copenhagen, Denmark. The mice were housed under standard laboratory conditions with different controlled lightening schedules and with free access to water and food.

All experiments with animals were performed in accordance with the guidelines of EU Directive 86/609/EEC approved by the Danish Council for Animal Experiments.

5.2. Antibodies

5.2.1. Primary antibodies—Polyclonal goat anti-cholera toxin IgG was obtained from List Biological Laboratories, Campbell, CA (cat. no. 703). Rabbit polyclonal anti-gastrin releasing peptide IgG was obtained from Abcam, Cambridge, UK. (cat. no. ab 22623-50). Polyclonal rabbit anti-melanopsin IgG was obtained from ABR Affinity Bioreagents, Golden, CO (cat. no. PAI-780) and polyclonal rabbit anti-vasoactive intestinal peptide IgG was a gift from Prof. J. Fahrenkrug (Bispebjerg Hospital, Copenhagen, Denmark), and polyclonal rabbit anti-vasopressin IgG was kindly provided by Prof. B.T. Pickering (University of Bristol, Bristol, UK).

5.2.2. Secondary antibodies—Affinity purified biotinylated anti-goat IgG and Vectastain ABC Elite kit (cat.no. PK-7200) were obtained from Vector Laboratories, Burlingame, CA (cat. no. BA-5000). Biotinylated swine anti-rabbit IgG was obtained form Dako, Glostrup, Denmark (cat. no. E0353).

5.3. Monitoring of circadian activity and temperature rhythms

Five adult wild type (C57BL/J6) mice and 5 homozygous *Crx*$^{-/-}$ were implanted with a TA-F40 radiotelemetry transmitter (Data Sciences International, St. Paul, MN). For analgesia, the animals were given a single dose of 10 ml/kg Hypnorm®/Dormicum® [0.16 mg/ml Fentanyl and 5 mg/ml Fluanisone (VetaPharma, Sherburn-in-Elmet, UK): 2.5 mg/ml Midazolam (Hameln Pharma, Hameln, Germany)] subcutaneously prior to the surgery, and 0.1 ml/kg Rimadyl® (Carprofen) once a day for the first 2 days after surgery. An incision, 1 cm in length, was made along the midline of the abdomen of the mice to obtain access to the intraperitoneal cavity. After insertion of the transmitter in the abdominal cavity, the incision

was closed with 5-0 nylon suture. The animals were kept in a 12 h light and 12 light/darkness schedule (12:12 L/D) for 2 months followed by continuous light (L/L) for 2 weeks, and then constant darkness (D/D) for 3 weeks.

The activity and temperature signals from the radiotelemetry transmitter were collected by a RMC-1 receiver (Data Sciences International) placed under the animals' cages. The receivers were connected to a Data Exchange Matrix (Data Sciences International) and connected to a Dataquest A.R.T.™ acquisition system.

5.4. Injection of cholera toxin tracer

Twenty animals were used for the tracing studies. Cholera toxin B subunit was obtained from List Biological Inc, Campbell, CA (cat. no. 103B). The cholera toxin tracer was dissolved in 0.05 M Tris buffer (pH 7.5) to a concentration of 10 μg/ml. The mice were intraperitoneally anesthetized with Hypnorm®/Dormicum® as described above and placed in a Kopf stereotaxic frame. The needle of a 5 μl Hamilton syringe was inserted into the corpus vitreum, and 1.5 μl of the cholera tracer was injected. After injection, the needle was left in the eye for 5 min. Postoperatively, the animals were pain treated with Rimadyl (0.1 ml/kg) subcutaneously. Animals were allowed to survive from 6 h to 14 days before perfusion fixation.

5.5. Perfusion fixation

Tracer injected mice and mice used for immunohistochemistry were anesthetized with Hypnorm®/Dormicum® as described above and transcardially perfused, firstly with phosphate buffered saline (PBS) to which 15.000 I.U. of Heparin per liter was added. This was followed by perfusion with 4% paraformaldehyde in 0.1 M phosphate buffer (pH 7.4) for 10 min. The brains and eye balls were removed and post fixed in the same fixative over night. The tissues were then cryoprotected in 30% sucrose in PBS for 2 days, frozen in crushed carbon dioxide and stored at −80 °C.

Some mice were perfused with 2.5% glutaraldehyde in 0.1 M phosphate buffer. The eyes were removed and after osmification, dehydrated and embedded in Epon®. Two μm thick sections were cut and stained with toluidine blue.

5.6. Immunohistochemical detection of the cholera toxin tracer

Three wild type and *Crx*$^{-/-}$ mice were used for immunohistochemical visualization of each peptide. Cryostat sections, 100 μm in thickness, were cut and placed in PBS. The sections were then washed in PBS for 3×5 min and the peroxidase activity was blocked in a 1% hydrogen peroxide in PBS for 10 min followed by washing for 10 min in incubation buffer (1% bovine serum albumin and 0.3% Triton X-100 in PBS). Unspecific binding was inhibited by incubation of the sections in 5% normal swine serum diluted in PBS for 30 min. This was followed by incubation in the primary antibody, polyclonal goat anti-cholera toxin IgG diluted 1:5,000 in incubation buffer. The sections were then washed 3×10 min in washing buffer (PBS with 0.25% bovine serum albumin and 0.1% Triton X-100) followed by incubation for 1 h in affinity purified biotinylated anti-goat IgG diluted 1/500 in incubation buffer. The sections were then washed 10 min in washing buffer, 10 min in PBS and again 10 min in washing buffer followed by incubation in ABC-Vectastain diluted 1/100 in washing buffer. After washing for 10 min in washing buffer and 10 min in 0.05 M Tris (pH 7.6), peroxidase activity was revealed by incubation in 1.4 mM diaminobenzidine (Sigma, Steinheim, Germany) and 0.01% H_2O_2 in 0.05 M Tris (pH 7.6) for 3–15 min. The reaction was terminated by washing the sections in PBS followed by deionized water. Finally, the sections were mounted on Superfrost Plus® glass slides and embedded in Pertex® (Histolab, Gothenburg, Sweden).

5.7. Immunohistochemistry

5.7.1. Detection of neuropeptides in the suprachiasmatic nuclei—Cryostat sections, 16 μm in thickness, were cut and mounted on Superfrost Plus® slides. The sections were washed 3×5 min in PBS and incubated in 5% swine serum in PBS for 30 min. The sections were then incubated in the primary antisera, raised against polyclonal rabbit anti-gastrin releasing peptide, polyclonal rabbit anti-vasoactive intestinal pep-tide or polyclonal rabbit anti-vasopressin, diluted 1:1,000 in incubation buffer. After washing for 3×5 min in washing buffer, sections were incubated in biotinylated anti-rabbit IgG, followed by incubation in ABC-Vectastain; chromogenic detection of peroxidase activity was performed as described above.

Acknowledgments

This study was supported by the Lundbeck Foundation, the Danish Medical Research Council (grant number 271-07-0412), the Novo Nordisk Foundation, the Carlsberg Foundation, Fonden til Lægevidenskabens Fremme, Simon Fougner Hart-manns Familiefond, the Danish Eye Health Society (Værn om Synet), and the Division of Intramural Research of the Eunice Kennedy Shriver National Institute of Child Health and Human Development, NIH. The authors wish to express their appreciation to Dr. Connie Cepko for providing the *Crx*$^{-/-}$ mice.

References

Abrahamson EE, Moore RY. Suprachiasmatic nucleus in the mouse: retinal innervation, intrinsic organization and efferent projections. Brain Res. 2001; 916:172–191. [PubMed: 11597605]

Berson DM, Dunn FA, Takao M. Phototransduction by retinal ganglion cells that set the circadian clock. Science. 2002; 295:1070–1073. [PubMed: 11834835]

Chen S, Wang QL, Nie Z, Sun H, Lennon G, Copeland NG, Gilbert DJ, Jenkins NA, Zack DJ. *Crx*, a novel Otx-like paired-homeodomain protein, binds to and transactivates photoreceptor cell-specific genes. Neuron. 1997; 19:1017–1030. [PubMed: 9390516]

Chou TC, Bjorkum AA, Gaus SE, Lu J, Scammell TE, Saper CB. Afferents to the ventrolateral preoptic nucleus. J Neurosci. 2002; 22:977–990. [PubMed: 11826126]

Chou TC, Scammell TE, Gooley JJ, Gaus SE, Saper CB, Lu J. Critical role of dorsomedial hypothalamic nucleus in a wide range of behavioral circadian rhythms. J Neurosci. 2003; 23:10691–10702. [PubMed: 14627654]

Czeisler CA, Shanahan TL, Klerman TL, Martens H, Brotman DJ, Emens JS, Klein T, Rizzo JF. Suppression of melatonin secretion in some blind patients by exposure to bright light. N Engl J Med. 1995; 332:6–11. [PubMed: 7990870]

David-Gray ZK, Janssen JWH, DeGrip WJ, Nevo E, Foster RG. Light detection in a 'blind' mammal. Nat Neurosci. 1998; 1:655–656. [PubMed: 10196579]

Doyle S, Menaker M. Circadian photoreception in vertebrates. Cold Spring Harb Symp Quant Biol. 2007; 72:499–508. [PubMed: 18419310]

Foster RG. Shedding light on the biological clock. Neuron. 1998; 20:829–832. [PubMed: 9620688]

Foster RG, Hankins MW. Non-rod, non-cone photoreception in the vertebrates. Prog Retin Eye Res. 2002; 21:507–527. [PubMed: 12433375]

Foster RG, Soni BG. Extraretinal photoreceptors and their regulation of temporal physiology. Rev Reprod. 1998; 3:145–150. [PubMed: 9829548]

Freedman MS, Lucas RJ, Soni B, von Schantz M, Muñoz M, David-Gray Z, Foster R. Regulation of mammalian circadian behavior by non-rod, non-cone, ocular photoreceptors. Science. 1999; 284:502–504. [PubMed: 10205061]

Fu Y, Liao HW, Do MTH, Yau KW. Non-image-forming ocular photoreception in vertebrates. Curr Opion Neukrobiol. 2005; 15:415–422.

Furukawa T, Morrow EM, Cepko CL. *Crx*, a novel Otx-like photoreceptor-specific expression and regulates photoreceptor differentiation. Cell. 1997; 91:531–541. [PubMed: 9390562]

Furukawa T, Morrow EM, Li T, Davis FC, Cepko CL. Retinopathy and attenuated circadian entrainment in *Crx*-deficient mice. Nat Genet. 1999; 23:466–470. [PubMed: 10581037]

Glynn EF, Chen J, Mushegian AR. Detecting periodic patterns in unevenly spaced gene expression time series using Lomb–Scargle periodograms. Bioinformatics. 2006; 22:310–316. [PubMed: 16303799]

Hankins MW, Peirson SN, Foster RG. Melanopsin: an exciting photopigment. Trends Neurosci. 2008; 31:27–36. [PubMed: 18054803]

Hannibal J, Møller M, Ottersen OP, Fahrenkrug J. Pituitary adenylate activating polypeptide (PACAP) and glutamate are co-stored in the retinohypothalamic tract. J Comp Neurol. 2000; 418:147–155. [PubMed: 10701440]

Hattar S, Liao HW, Takao M, Berson DM, Yau KW. Melanopsin-Containing Retinal Ganglion Cells: Architecture, projections, and intrinsic photosensitivity. Science. 2002; 295:1065–1070. [PubMed: 11834834]

Hattar S, Kumar V, Park A, Tong V, Tung J, Yau KW, Berson DM. Central Projections of Melanopsin-Expressing Retinal Ganglion Cells in the Mouse. J Comp Neurol. 2006; 497:326–349. [PubMed: 16736474]

Jessop DC, Eckland DJA, Todd K, Lightman SL. Osmotic regulation of hypothalamoneurointermediate lobe corticotrophin-releasing factor-41 in the rat. J Endocrinol. 1989; 120:119–124. [PubMed: 2537368]

Kappers JA. The development, topographical relations and innervation of the epiphysis cerebri in the albino rat. Z Zellforsch Mikrosk Anat. 1960; 52:163–215. [PubMed: 13751359]

Klein DC, Smoot R, Weller JL, Higa S, Markey SP, Creed GJ, Jacobowitz DM. Lesions of the paraventricular nucleus area of the hypothalamus disrupt the suprachiasmatic leads to spinal cord circuit in the melatonin rhythm generating system. Brain Res Bull. 1983; 10:647–652. [PubMed: 6307491]

Klein DC, Coon SL, Roseboom PH, Weller JL, Bernard M, Gastel JA, Zatz M, Iuvone PM, Rodriguez RI, Begay V, Falcon J, Cahill GM, Cassone VM, Baler R. The melatonin rhythm-generating enzyme: molecular regulation of serotonin N-acetyltransferase in the pineal gland. Rec Prog Horm Res. 1997; 52:307–357. [PubMed: 9238858]

Korf HW, von Gall C, Stehle J. The circadian system and melatonin: lessons from rats and mice. Chronobiol Int. 2003; 20:697–710. [PubMed: 12916721]

Larsen PJ, Enquist LW, Card JP. Characterization of the multisynaptic neuronal control of the rat pineal gland using viral transneuronal tracing. Eur J NeuroSci. 1998; 10:128–145. [PubMed: 9753120]

Lomb N. Least-squares frequency analysis of unequally spaced data. Astrophys Space Sci. 1976; 39:447–462.

Lu J, Zhang YH, Chou TC, Gaus SE, Elmquist JK, Shiromani P, Saper CB. Contrasting effects of ibotenate lesions of the paraventricular nucleus and subparaventricular zone on sleep-wake cycle and temperature regulation. J Neurosci. 2001; 21:4864–4874. [PubMed: 11425913]

Lucas RH, Hattar S, Takao M, Berson DM, Foster RG, Yau KW. Diminished pupillary light reflex at high irradiances in melanopsin-knokout mice. Science. 2003; 299:245–247. [PubMed: 12522249]

Morin LP. The circadian visual system. Brain Res Rev. 1994; 19:102–127. [PubMed: 7909471]

Morrow EM, Furukawa T, Raviola E, Cepko CL. Synaptogenesis and outer segment formation are perturbed in the neural retina of Crxmutant mice. BMC Neurosci. 2005; 6:5. www.biomedcentral.com/1471-2202/6/5. [PubMed: 15676071]

Munch IC, Møller M, Larsen PJ, Vrang N. Light-induced c-Fos expression in suprachiasmatic nuclei neurons targeting the paraventricular nucleus of the hamster hypothalamus: phase dependence and immunochemical identification. J Comp Neurol. 2002; 442:48–62. [PubMed: 11754366]

Møller M, Baeres FMM. The anatomy and innervation of the mammalian pineal gland. Cell Tissue Res. 2002; 309:139–150. [PubMed: 12111544]

Nishida A, Furukawa A, Koike C, Tano Y, Aizawa S, Matsuo I, Furukawa T. Otx2 homeobox gene controls retinal photoreceptor cell fate and pineal gland development. Nat Neurosci. 2003; 6:1255–1263. [PubMed: 14625556]

Okamura H. Clock genes in cell clocks: roles, actions, and mysteries. J Biol Rhythms. 2004; 19:388–399. [PubMed: 15534319]

Panda S, Sato TK, Castrucci AM, Rollag MD, DeGrip WJ, Hogenesch JB, Provencio I, Kay SA. Melanopsin (Opn4) requirements for normal light-induced circadian phase shifting. Science. 2002; 298:2213–2216. [PubMed: 12481141]

Panda S, Provencio I, Tu DC, Pires SS, Rollag MD, Castrucci AM, Pletcher MT, Sato TK, Wiltshire T, Andahazy M, Kay SA, Van Gelder RN, Hogenesch JB. Melanopsin is required for non-image-forming photic responses in blind mice. Science. 2003; 301:525–527. [PubMed: 12829787]

Peng GH, Chen S. *Crx* activates opsin transcription by recruiting HAT-containing coactivators and promoting histone acetylation. Hum Mol Genet. 2007; 16:2433–2452. [PubMed: 17656371]

Provencio I, Rodriguez IR, Jiang G, Hayes WP, Moreira EF, Rollag MD. A novel human opsin in the inner retina. J Neurosci. 2009; 20:600–605. [PubMed: 10632589]

Rath MF, Morin F, Shi Q, Klein DC, Møller M. Ontogenetic expression of the Otx2 and *Crx* homeobox genes in the retina of the rat. Exp Eye Res. 2007; 85:65–73. [PubMed: 17467693]

Refinetti R. Effects of suprachiasmatic lesions on temperature regulation in the golden hamster. Brain Res Bull. 1995; 36:81–84. [PubMed: 7882054]

Ruby NF, Brennan TJ, Xie X, Cao V, Franken P, Heller HC, O'Hara BF. Role of melanopsin in circadian responses to light. Science. 2002; 298:2211–2213. [PubMed: 12481140]

Ruggiero L, Allen CN, Brown RL, Robinson DW. The development of melanopsin containing retinal ganglion cells in mice with early retinal degeneration. Eur J NeuroSci. 2009; 29:359–367. [PubMed: 19200239]

Saper CB, Lu J, Chou TC, Gooley J. The hypothalamic integrator for circadian rhythms. Trends Neurosci. 2005; 28:152–157. [PubMed: 15749169]

Scargle JD. Studies in astronomical time series analysis. II. Statistical aspects of spectral. Astrophys J. 1982; 263(835):853.

Scheer FA, Pirovano C, van Someren EJ, Buijs RM. Environmental light and suprachiasmatic nucleus interact in the regulation of body temperature. Neuroscience. 2005; 132:465–477. [PubMed: 15802197]

Semo M, Peirson S, Lupi D, Lucas RJ, Jeffery G, Foster RG. Melanopsin retinal ganglion cells and the maintenance of circadian and pupillary respons to light an aged rodless/coneless (rd/rd cl) mice. Eur J NeuroSci. 2003; 17:1793–1801. [PubMed: 12752778]

Sugiyama S, Di Nardo AA, Aizawa S, Matsuo I, Volovitch M, Prochiantz A, Hensch TK. Experience-dependent transfer of Otx2 homeoprotein into the visual cortex activates postnatal plasticity. Cell. 2008; 134:508–520. [PubMed: 18692473]

Tosini G, Aguzzi J, Bullock NM, Liu C, Kasamatsu M. Effect of photoreceptor degeneration on circadian photoreception and free-running period in the Royal College of Surgeons rat. Brain Res. 2007; 1148:76–82. [PubMed: 17382912]

Viney TJ, Balint K, Hillier D, Siegert S, Boldogkoi Z, Enquist LW, Meister M, Cepko CI, Roska B. Local retinal circuits of melanopsin-containing ganglion cells identified by transsynaptic viral tracing. Curr Biol. 2007; 17:981–988. [PubMed: 17524644]

Vrang N, Larsen PJ, Mikkelsen JD. Direct projection from the suprachiasmatic nucleus to hypophysiotrophic corticotropin-releasing factor immunoreactive cells in the paraventricular nucleus of the hypothalamus demonstrated by means of Phaseolus vulgarisleucoagglutinin tract tracing. Brain Res. 1995; 684:61–69. [PubMed: 7583205]

Warren EJ, Allen CN, Brown RL, Robinson DW. Intrinsic light responses of retinal ganglion cells projecting to the circadian system. Eur J NeuroSci. 2003; 17:1727–1735. [PubMed: 12752771]

Yanovski J, Witcher J, Adler N, Markey S, Klein DC. Stimulation of the paraventricular nucleus area of the hypothalamus elevates urinary 6-hydroxymelatonin during daytime. Brain Res Bull. 1987; 19:129–133. [PubMed: 3651836]

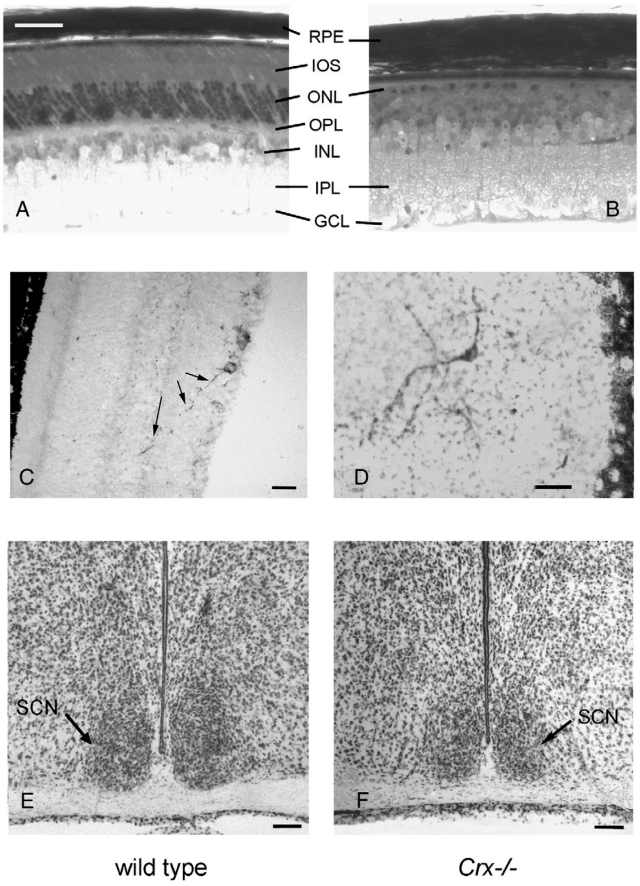

Fig. 1.

(A and B) Photomicrographs of 2 μm thick Epon-embedded, toluidine blue stained, sections of the wild type mouse (A) and the *Crx*$^{-/-}$ knock out mouse (B). Note the thinning of the retina in the *Crx*$^{-/-}$ mouse due to the missing inner and outer segments (IOS) of the photoreceptors. (C and D) Melanopsin-immunoreactive cells in the retina of the wild type mouse (C) and the *Crx*$^{-/-}$ knock out mouse (D). A long melanopsin-immunoreactive process (arrows) from a ganglion cell perikaryon is penetrating into the outer nuclear layer. The section of the retina in the *Crx*$^{-/-}$ mouse is cut in a tangential plane. (E and F) Photomicrograph of Nissl stained 40 μm thick coronal cryostat sections of the suprachiasmatic nuclei (SCN), located above the optic chiasm, of the control mouse (E) and the *Crx*$^{-/-}$ mouse (F). GCL=ganglion cell layer, INL=inner nuclear layer, IPL=inner plexiform layer, ONL=outer nuclear layer, OPL=outer plexiform layer, RPE=retinal pigment epithelium, SCN=suprachiasmatic nucleus. Bars; A and B=40 μm, C and D=25 μm, E and F=100 μm.

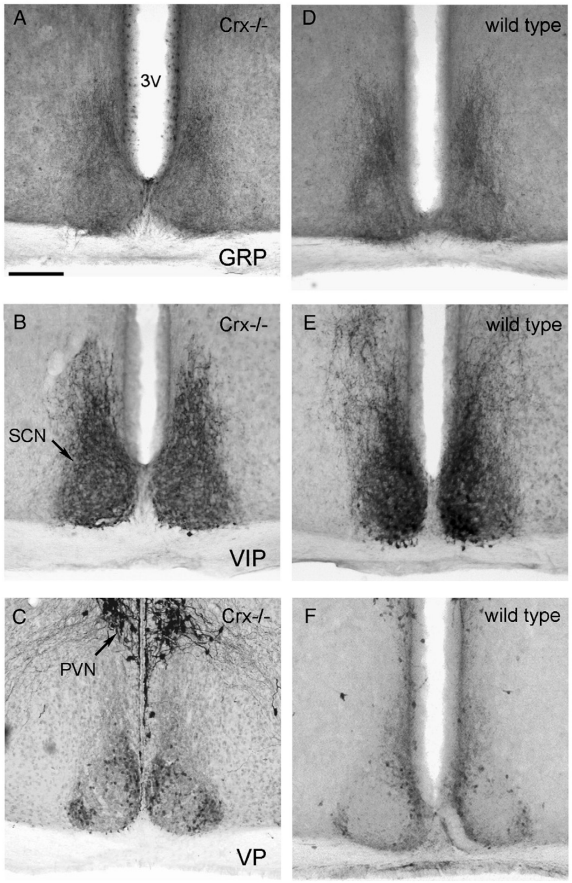

Fig. 2.

Photomicrographs of the suprachiasmatic nuclei of the *Crx*$^{-/-}$ (left column) and wild type (right column) mouse. The sections have been immunohistochemically reacted for gastrin releasing peptide (GRP, A and D), vasoactive instestinal peptide (VIP, B and E), and vasopressin (VP, Figs. 2C and F). 3V=third ventricle, PVN=paraventricular nucleus, SCN=suprachiasmatic nucleus. Bar=200 μm.

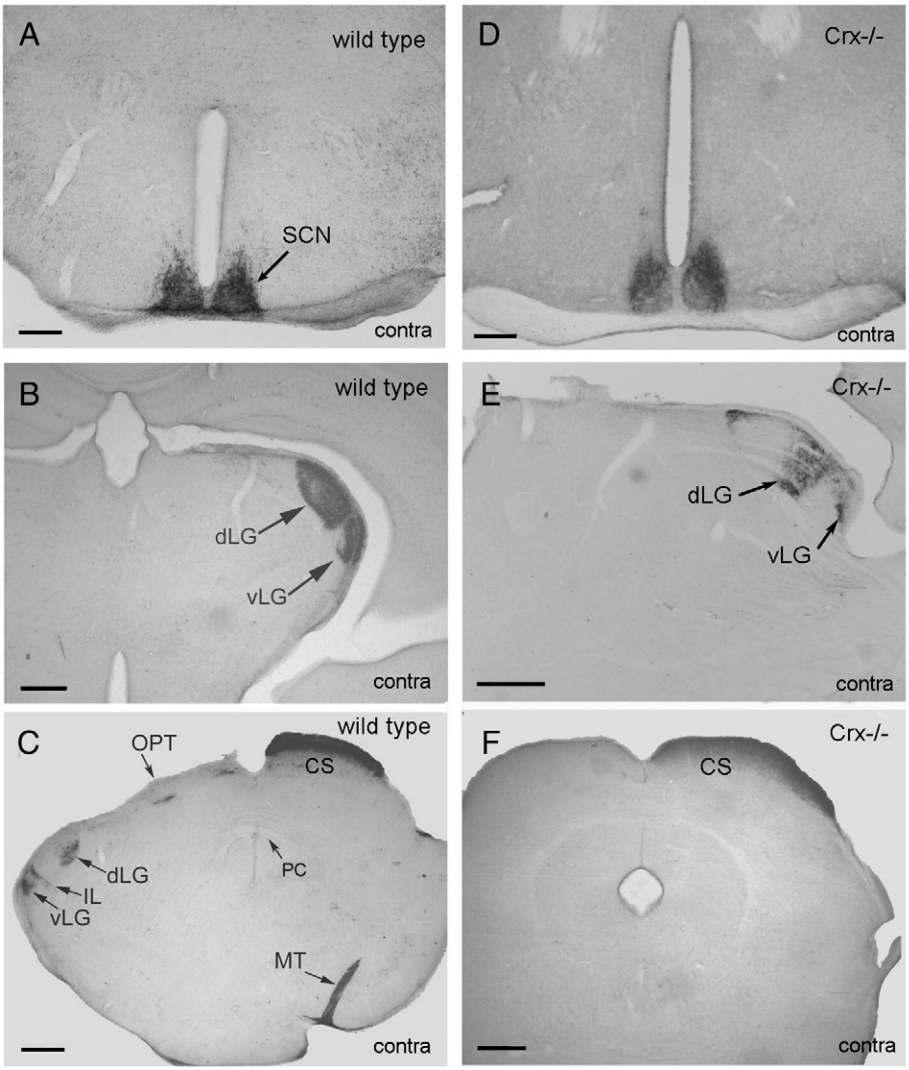

Fig. 3.

Montage of frontal sections of wild type mouse (left column) and *Crx*$^{-/-}$ mouse (right column) in which cholera toxin tracer has been injected into the eye and transported for 4 days before perfusion fixation of the animal. A dense innervation of the suprachiasmatic nuclei (SCN) is seen both in the wild type and *Crx*$^{-/-}$ mouse (A and D). In more caudal parts of the diencephalon a dense innervation of the ventral (vLG) and dorsal (dLG) lateral geniculate nucleus (B and E) is seen on the contralateral side of the injection. The tracer terminates in a large terminal field in the superior colliculus (CS) contralateral to the injection (C and F). Ipsilateral to the injection, the innervation of the lateral geniculate nucleus is less intense (C). Il=intergeniculate leaflet, MT=medial terminal nucleus, OPT=nucleus of the optic tract, PC=posterior commissure. Bars=200 μm (A and D), 100 μm (B, C, E, and F).

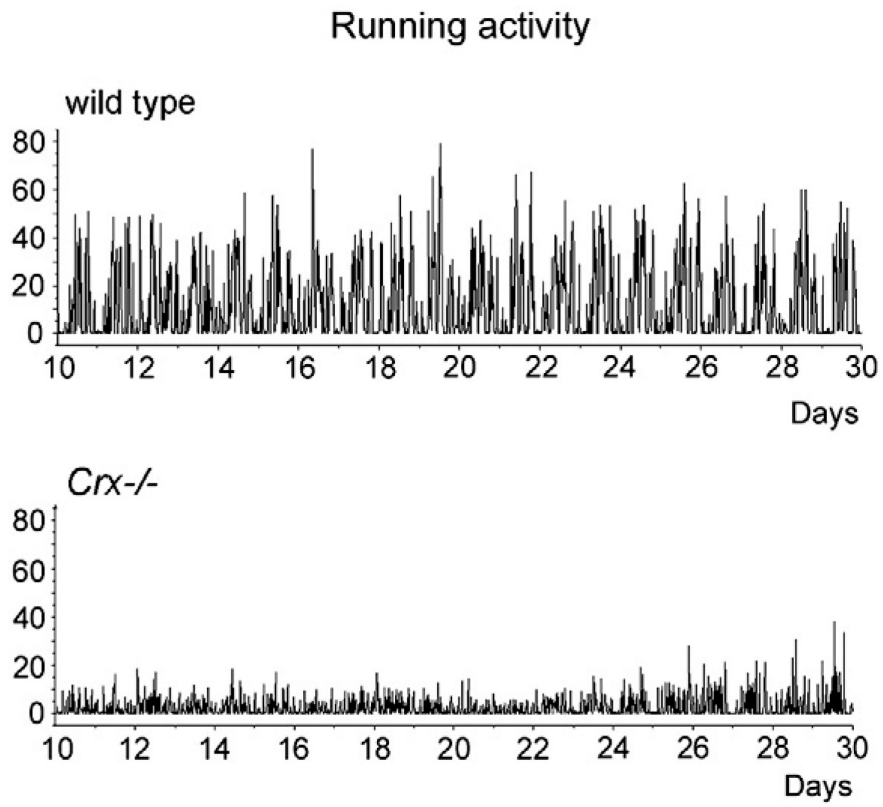

Fig. 4.

Telemetric registration of "running activity" in the wild type and the $Crx^{-/-}$ mouse for 20 days. The ordinate is in arbitrary units.

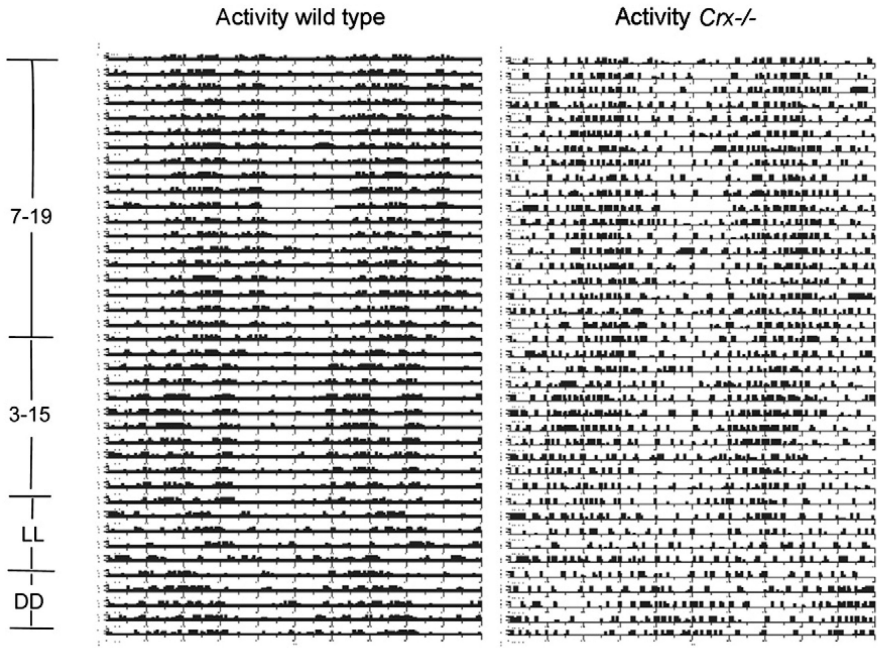

Fig. 5.

Actogram showing telemetric registration for 80 days of the "running activity" of a representative control mouse and a $Crx^{-/-}$ mouse. For the first 40 days, the animals were exposed to a 12L:12D light regime (lights on at 7 a.m.). For the following 20 days, the light regime was phase advanced with 4 h (lights on at 3 a.m. and of at 3 p.m.). This was followed by continuous light for 10 days (LL). Finally, the animals were kept in constant darkness for 10 days (DD).

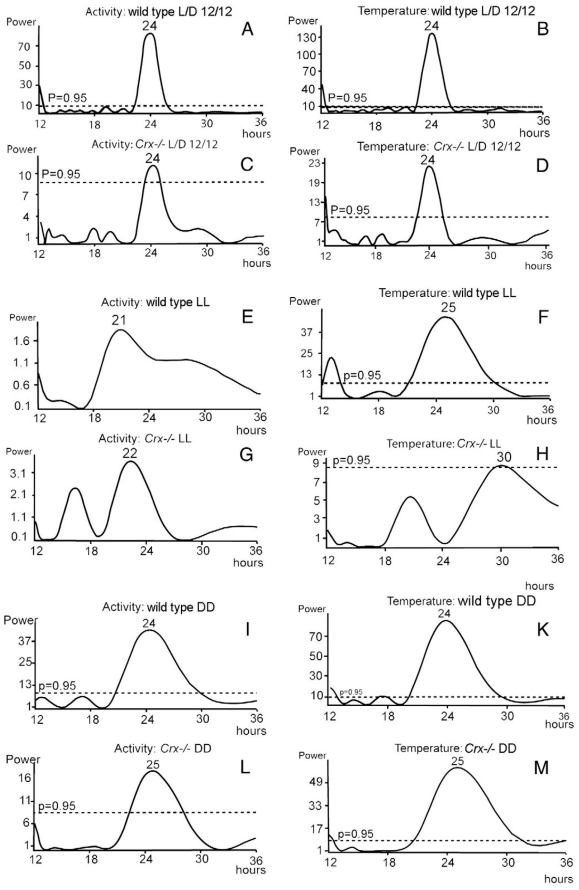

Fig.6.

Lomb–Scargle power spectral analysis of the activity periods (left column) and temperature periods (right column) in wild type mice (A, B, E, F, J, and K) and $Crx^{-/-}$ mice (C, D, G, H, L, and M). For more detailed description see Results.

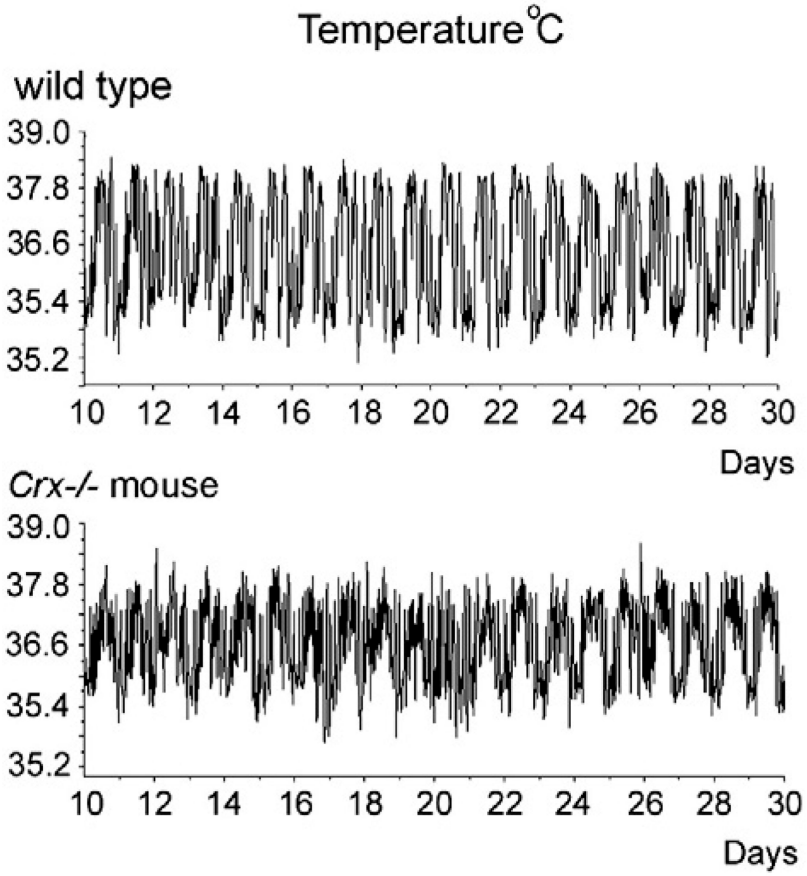

Fig. 7.
Telemetric monitoring of circadian temperature curves in a control and $Crx^{-/-}$ mouse for 20 days. Ordinate is the temperature in Celsius degrees.

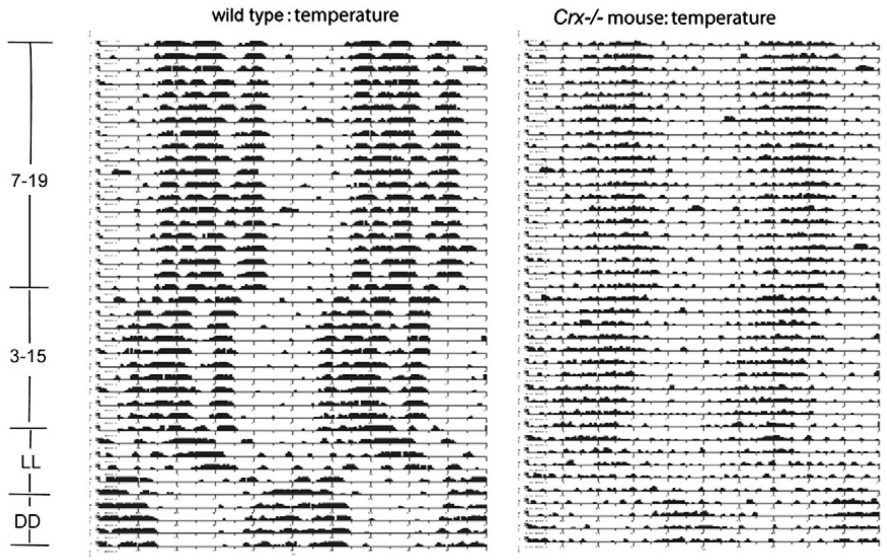

Fig. 8.

Core body temperature plot of a control and *Crx*$^{-/-}$ mouse monitored for 80 days. For the first 40 days, the animals were exposed to a 12 L:12D light regime (lights on at 7 a.m.). For the following 20 days, the light regime was phase advanced with 4 h (lights on at 3 a.m. and of at 3 p.m.). This was followed by continuous light for 10 days (LL). Finally, the animals were kept in constant darkness for 10 days (DD).

Table 1

Activity of wild type and *Crx*$^{-/-}$ mice from day 10 to 30

	Wild type	*Crx*$^{-/-}$	95% Confidence intervals
Mesor (95% confidence interval)	11.7 [11.0–12.3]	2.63 [2.34–2.91]	
Temperature wild type and *Crx*$^{-/-}$ mice from day 10 to 30			
	Wild type	*Crx*$^{-/-}$	
Mesor (95% confidence interval)	36.4 [36.4–36.5]	36.3 [36.3–36.4]	